

A Novel Approach for Experimental Earthquake Engineering Utilizing Mirror Reflections of Point Clouds Collected by Laser Scanner

Shakhzod Takhirov¹^a, Mukhady Israilov² and Sultan Kudratov³^b

¹Department of Civil and Environmental Engineering, University of California, Berkeley, U.S.A.

²Joint Research Institute of Russian Academy of Sciences (KNII-RAN), Grozny, Russian Federation

³Department of Information Technologies, Tashkent University of Information Technologies, Tashkent, Uzbekistan

Keywords: Laser Scanning, Point Cloud, Experimental Earthquake Engineering, Mirror Reflection, 4D Surface Tracking, Surface Deformation.

Abstract: A laser scanner is an optical instrument that emits laser beams toward objects surrounding the scanner and measures the location of the objects' points in space. As a result, it collects the so-called point clouds. In experimental earthquake engineering, the laser scanners have been used in many applications. In quasi-static testing, they used for four-dimensional tracking of the test specimen's condition in three spatial coordinates and time. When a single scanner is used, the object's rear surface is in shadow zone and as such, the points of the rear surface are not collected. To acquire the point cloud of the object's rear side two commonly used options are utilized. In Option 1, several scanners working in parallel can be deployed. In Option 2, the same scanner can be moved to other positions to cover the shadow zones. Option 1 represents an expensive option that requires an investment in two or more scanners, finding a way of triggering them simultaneously, and time required for registration of the point clouds collected by several scanners. The main shortcoming of Option 2 is that it does not allow simultaneous scans from both sides and registration of the laser scans from many different points can be time consuming. To overcome shortcomings of these two options, this paper introduces a novel approach (Option 3) of using several mirrors strategically placed in respect to a single scanner to cover the shadow zones with a single scanner and from the same position. To ensure cost-effectiveness of the approach, this research was focused on the utilization of affordable and commonly used rear-reflective mirrors. This paper investigates the point clouds obtained from the mirror reflections and quantifies the quality of these data by estimating accuracy and reliability of the reflected point cloud data. The theoretical estimates were verified by laser scanning of sample test specimens.

1 INTRODUCTION

A laser scanner is an optical instrument that emits laser beams toward objects surrounding the scanner and measures the duration of the time-of-flight (TOF) of the laser beams that are reflected back. The distance to the object is computed by multiplying this duration by the speed of light in the air. Obviously, only the points of the object's surface visible from the location of the scanner will be collected. The object's rear side is not visible, and this will result in a shadow zone in the point cloud where the points cannot be collected from this particular location of the laser

scanner. Situations where a reflective surface of any kind is present in close proximity to the laser scanner are quite common as presented in Figure 1. In this case, the laser acquires the points representing a rear portion of the object that would not be detected by a laser scanner otherwise. This paper investigates the point clouds obtained from the mirror reflections and quantifies the quality of these data by estimating accuracy and reliability of the reflected point cloud data.

^a <https://orcid.org/0000-0002-4396-7946>

^b <https://orcid.org/0000-0001-9650-4331>



Figure 1: Laser scanning next to a mirror at a department store (point cloud).

2 MOTIVATION

In experimental earthquake engineering the laser scanners have been used in many applications (see Takhirov, 2010; Mosalam, Takhirov, and Hashemi, 2009; Mosalam, Takhirov, and Park, 2014, as representative examples). It is used for four-dimensional tracking of the test specimen's condition in three spatial coordinates and time. When a single scanner is used, the object's rear surface is in shadow zone and the points of the rear surface are not collected. To acquire the point cloud of the object's rear side two options can be used. In Option 1, several scanners working in parallel can be deployed. In Option 2, the same scanner can be moved to other positions to cover the shadow zones. Option 1 is expensive as it requires an investment in two or more scanners, finding a way of triggering them simultaneously, and a registration of the point clouds collected by several scanners. The main shortcoming of Option 2 is that it does not allow simultaneous scans from both sides, and a registration of the laser scans from many different points can be time consuming. This paper introduces a novel approach of using several mirrors strategically placed in respect to a single scanner to cover the shadow zones with a single scanner and from the same position.

3 GENERAL COMMENTS ABOUT THE LIGHT REFLECTION PROBLEM

For simplicity, let us assume that the coordinate system is selected in such a way that the mirror is located in the horizontal plane. We will assume that the imperfections of the mirror are negligible and as

such, the incident and the reflected rays remain in the same plane as presented in Figure 2.

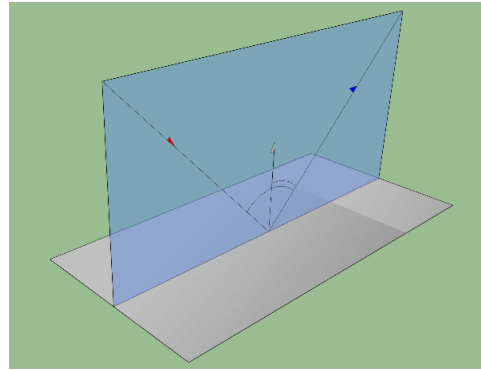


Figure 2: Trajectories of incident beam and beam reflected from horizontal surface remain in the same plane.

One of the main principles in optics is that the incident and reflected angles will be the same in respect to the normal of the plane from which the reflection occurs (Lekner, 1987). Therefore, all trajectories of the incident and reflected laser beams will be in a plane that contains the focal center of the scanner (emitting point) and the location of the point measured by the laser scanner. As discussed above this plane is orthogonal to the plane of the mirror.

4 EXPERIMENTAL SETUP AND SUBSETS OF COLLECTED POINT CLOUD

The quality of the reflected point cloud was investigated in the following experimental setup. Several tinted glass globes, two prismatic shapes (one wooden block and one cardboard box) and several high-definition laser targets (HDLT) were strategically placed inside an experimental room. The laser scanner was installed in such a way that all objects were visible from the scanner's location and were visible in the mirror's reflection. To minimize the effect of the reflectivity of the shiny glass surface, the globes were spray painted with a flat grey paint. The mirror's location in space was identified by using three HDLTs that are commonly used for stitching the laser scans. In addition, three HDLTs were placed on the walls of the room. Twelve targets were placed on a large piece of thick plywood. Special plywood with a high flatness tolerance was selected for this purpose. A photo of the experimental setup is presented in Figure 3. The corresponding point cloud is presented in Figure 4. The scans were performed with Scan

Station C10 (Leica Geosystems AG, 2011), Scan Station P40 (Leica Geosystems AG 2019), both from Leica Geosystems, Focus S-350 from FARO Technologies Inc (FARO Technologies Inc., 2020) and TX6 scanner form Trimble (Trimble, 2016). For the purpose of this paper, the results for one of the scanners (namely, Scan Station C10) are discussed in more detail.

It is worth noting that usage of the HDLTs was crucial for achieving the objectives of the paper. Earlier it was observed that the mid-range (up to 200 m) laser scanners from Leica Geosystems produce a noisier point cloud than a close-range high-accuracy laser scanner (Takhirov, 2010). Nevertheless, averaging the point cloud brings it much closer to the actual surface. In addition, it was shown that while the nominal accuracy of individual point cloud acquisition is ± 6 mm at 50 m range (Leica Geosystems AG, 2011 and 2019) the accuracy of HDLT's acquisition is less than 1 mm (Takhirov, 2008). The high accuracy of the flat black and white geometric patterns similar to the HDLTs used in this paper was reported earlier by many other authors (see Janßen et al, 2019 as a representative example).



Figure 3: Photo of experimental setup.

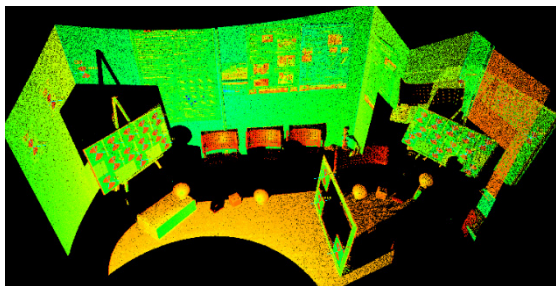


Figure 4: Corresponding point cloud.

The initial data manipulation was conducted in Cyclone (Leica Geosystems AG, 2018). The acquired point cloud was separated in three subsets. First, the subset consisting of the point cloud excluding the

mirror reflection was separated. It was called 'Reality'. Second, the subset consisting of the point cloud behind the mirror surface was separated. It was called 'Reflection'. Third, the subset of the point cloud corresponding to the HDLTs on the mirror's front surface was separated. It was called 'Mirror'. To simplify the data manipulation, the coordinate system of the point cloud was changed in Cyclone [10] to have all the vertices of the mirror's targets in the plane $Y=0$. After all these preparations, the subsets were exported as ASCII files to be manipulated in the Matlab [MathWorks, 2016] environment. All subsets are presented in Figure 5. It was expected that a geometric transformation corresponding to the mirror reflection would result in consistent point clouds of the objects with actual surfaces completed by reflected point clouds. To improve the accuracy of mirror transformation vertices of the high-definition targets were used. The targets and their locations in respect to the mirror are presented in Figure 6.

In Figure 5 and Figure 6, the points related to Reality, Reflection and Mirror are presented in red, blue and green colors, respectively.

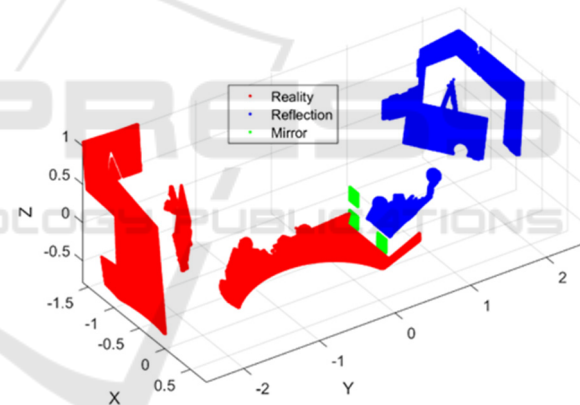


Figure 5: Point clouds.

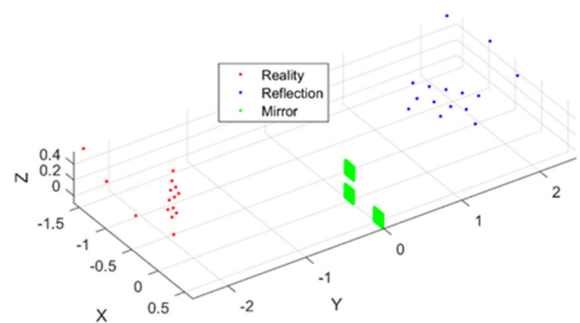


Figure 6: Vertices of targets.

5 GEOMETRIC TRANSFORMATION USED FOR THE REGISTRATION OF REAL AND REFLECTED CLOUDS

The mirror transformation of the point clouds based on the location of the front surface of the mirror resulted in a large error between the real and reflected targets. The error related to the assumption that the reflective surface is located on the front side of the mirror. In reality, consumer grade mirrors are manufactured as a large piece of glass with the reflective surface on its rear side as presented in Figure 7. When the laser beam comes into contact with the front side of the glass it refracts and changes its direction and velocity of propagation. Subsequently, the refracted laser beam reflects from the reflective surface and it refracts again while exiting the glass layer. Therefore, an offset needs to be introduced into the geometric transformation that will account for the thickness of the glass layer, d , and the refraction of the laser beams in the glass layer. It is obvious that the offset, b , will depend on the incidence angle of the incident laser beam. For the purpose of the paper, this offset was estimated by minimizing the distance between real and reflected targets. To this extent, an effective thickness of the glass that includes the refraction effect was obtained.

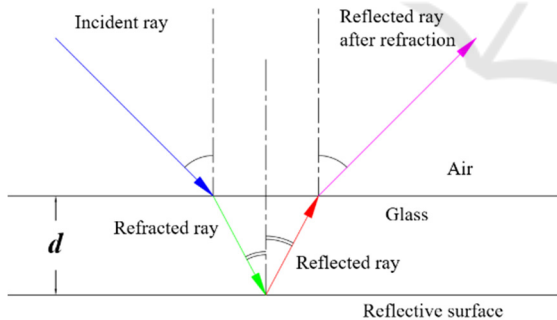


Figure 7: Mirror with a glass layer (consumer grade mirror).

The following procedure was used. To obtain a transformed point cloud of Reflection, (x_2, y_2, z_2) , a mirror geometric transformation was applied to Reflection point clouds (x_1, y_1, z_1) with an offset vector of $(0, b, 0)$:

$$\begin{bmatrix} x_2 \\ y_2 \\ z_2 \end{bmatrix} = \begin{bmatrix} 1 & 0 & 0 \\ 0 & -1 & 0 \\ 0 & 0 & 1 \end{bmatrix} \begin{bmatrix} x_1 \\ y_1 \\ z_1 \end{bmatrix} + \begin{bmatrix} 0 \\ b \\ 0 \end{bmatrix}$$

The glass thickness and refraction correction factor, b , was varied from 15 mm to -15 mm. For each value of b , the distances between the real and reflected targets were computed. The maximum variation of these distances was estimated by subtracting the minimum value from the maximum value. The result presented in Figure 8 shows that the smallest error occurs when $b = 8.405 \text{ mm}$. The procedure was used for the targets in close proximity to the mirror as shown in Figure 9. This offset value was used in combination with the mirror transformation to compare reality and reflection point clouds. The resultant registration is presented in Figure 10. All targets in 3D space are shown in Figure 6a and errors in the target locations are presented in Figure 11.

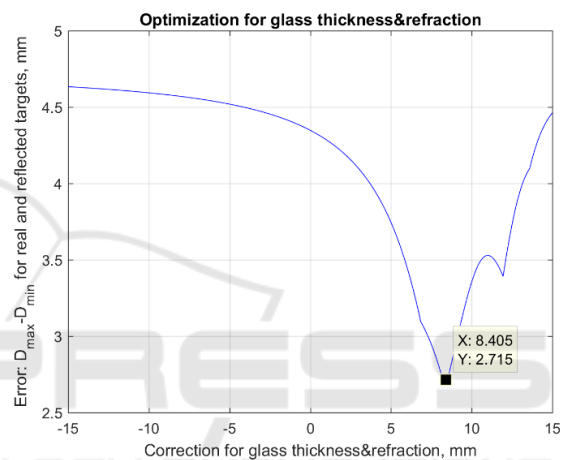


Figure 8: Minimization of error between real and reflected targets.

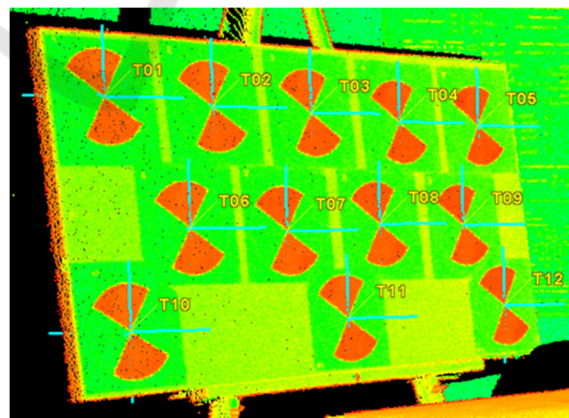


Figure 9: Only HDLTs in close proximity to the mirror were used for the optimization.

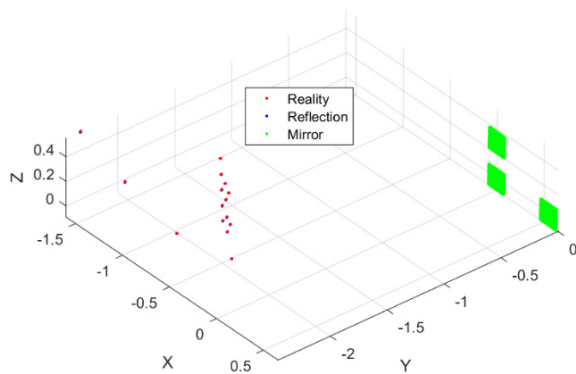


Figure 10: All targets in 3D space.

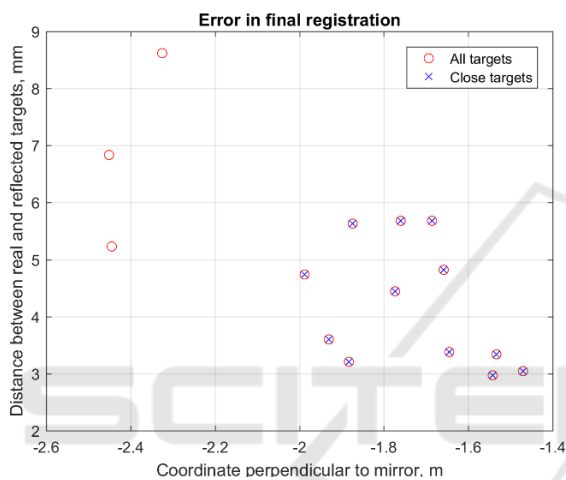


Figure 11: Distance between real and reflected targets: close targets have smaller distance.

The final registration resulted in a reflected point cloud with a reasonably good quality that complemented the point cloud collected by the scanner without the mirror. The overall view of the real and reflected point clouds combined in the final registration is presented in Figure 12. A horizontal section of the same registration showing a close matching of the two globes is presented in Figure 13. Figure 14 presents another horizontal section of the registration that shows closely matched point clouds for both prismatic shapes and a globe. A good correlation between point clouds of Reality and Reflection relative to the walls of the room is presented in Figure 15.

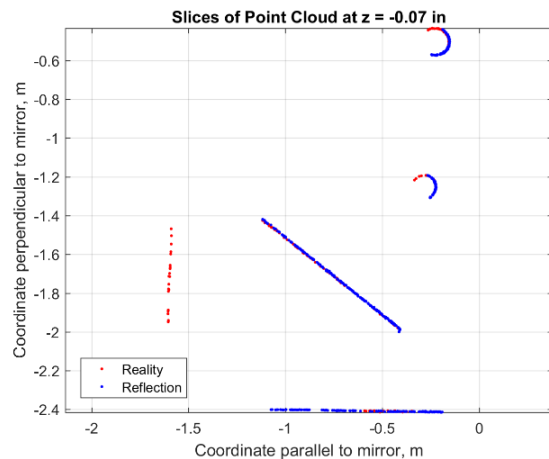


Figure 12: Registration of Reality and Reflection in 3D space.

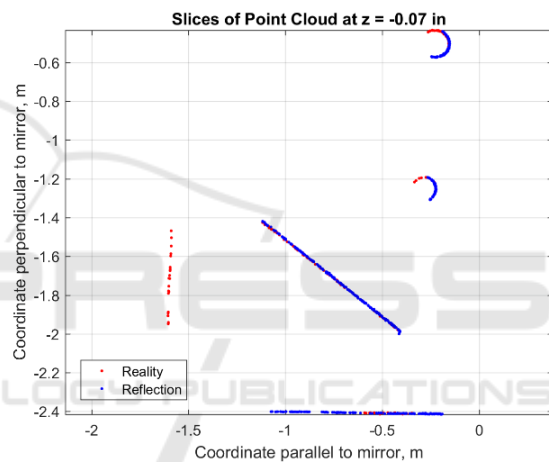


Figure 13: Horizontal slice of the registration at $Z = -0.07\text{m}$: two globes, surface with targets, two walls.

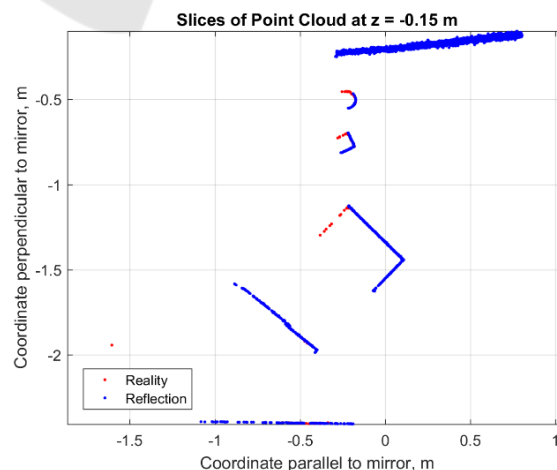


Figure 14: Horizontal slice of the registration at $Z = -0.15\text{m}$: a globe, two prismatic shapes, surface with targets, a wall.

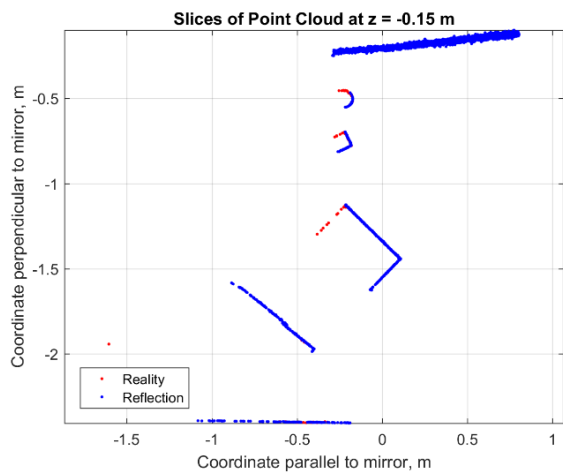


Figure 15: Horizontal section at $Z = 0.62$ m (two walls and a plywood with targets).

The same approach was used for registering real point clouds with the ones obtained from the reflection in the laser scans obtained by the TX6 scanner (Trimble, 2016). A typical experimental setup with the TX6 scanner is presented in Figure 16. Figure 17 presents the experimental setup with the P40 scanner, which was also used in this study.



Figure 16: Experimental setup with TX6 scanner.



Figure 17: Experimental setup with P40 scanner.

This approach was also used for registering the real point clouds with those reflected by the mirror in the case of the Focus S-350 scanner too. A typical result showing real and reflected point clouds stitched together based on this approach are presented in Figure 18.

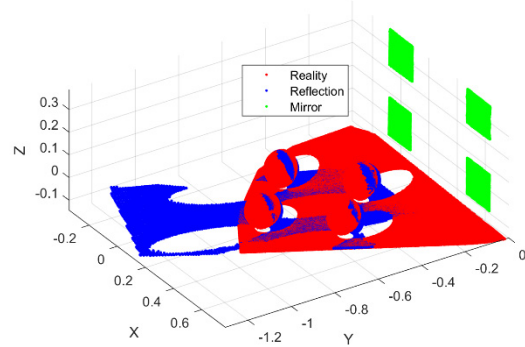


Figure 18: Registration of real and reflected point clouds for globes (Focus S-350 scanner).

This approach allows the registration of reflected point clouds with the real ones for more complex and irregular shapes as presented in Figure 19.

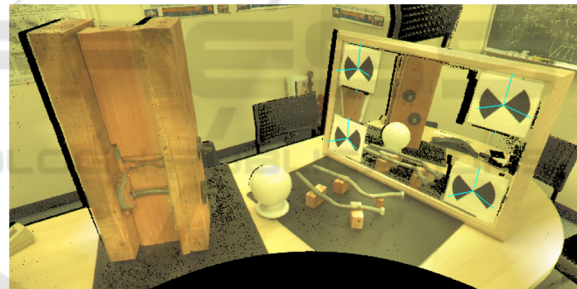


Figure 19: Laser scanning of complex shapes by utilizing the mirror approach.

In addition to a regular scanning of the objects, this approach can be used for 4D surface tracking of test specimens during their deformation under a test. If the position of the scanner is fixed for the duration of the test, the registration between the reflected and real point clouds needs to be done only once. The latter makes the approach quite valuable and cost effective for this kind of application and does not require having several scanners to capture the shadow zones.

The process of registration can be established and/or mathematically verified by an analytical formula based on geometry and the physics of reflection and refraction of laser beams. This portion of the research is ongoing and will be included in future publications.

6 CONCLUSIONS

This paper investigates the point clouds obtained from mirror reflections and quantifies the quality of these data by estimating accuracy and reliability of the reflected point cloud data. It is shown that the accuracy of the reflected point cloud will depend on the thickness of the front glass layer that is usually present in consumer grade mirrors. In addition, accuracy depends on the refraction effects and the angle of incident beams. In the particular case where the variation of the incident angles is limited, a simplified correction factor can be introduced that significantly improves the quality of the final registration. The correction factor is obtained by minimizing the error between the high-definition targets visible with and without the mirror during optimization of the registration process. In this case, it is shown that the overall error of the registration is less than 4 mm, which is acceptable for many applications. When the deformed shape of a test specimen is tracked in 3D over time (4D tracking), the scanner's position does not change and such, the registration discussed above needs to be done only once, let's say for the very first scan of the specimen's undeformed shape.

ACKNOWLEDGEMENTS

Special thanks are due to the Pacific Earthquake Engineering Research Center (PEER), UC Berkeley for providing access to Scan Station C10. Also, special thanks are due to Leica Geosystems for providing access to Scan Station P40 which was crucial for achieving the objectives of the paper. The authors would like to thank FARO Technologies Inc for providing access to Focus S-350. Special thanks are due to Sensor Fusion and Monitoring Technologies, LLC, for providing access to TX6 scanner from Trimble. The active participation of Dr. Gregory Walsh of Leica Geosystems in discussion of the project's objectives is greatly appreciated. Special thanks are due to Holly Halligan of UC Berkeley for editing the paper.

REFERENCES

FARO Technologies Inc. (2020). <https://www.faro.com/products/construction-bim/faro-focus/>.
 Janßen, J., Medic, T., Kuhlmann H., and Holst, C. (2019). Decreasing the Uncertainty of the Target Center Estimation at Terrestrial Laser Scanning by Choosing

the Best Algorithm and by Improving the Target Design. *Remote Sensing*. 11, 845; doi:10.3390/rs11070845.
 Leica Geosystems AG (2011). Leica ScanStation C10. https://w3.leica-geosystems.com/downloads123/hds/hds/ScanStation%20C10/brochures-datasheet/Leica_ScanStation_C10_DS_en.pdf.
 Leica Geosystems (2018). Cyclone Version 9.2.1.
 Leica Geosystems AG (2019). Leica ScanStation P40/P30 - High-Definition 3D Laser Scanning Solution. <https://leica-geosystems.com/en-us/products/laser-scanners/scanners/leica-scanstation-p40--p30>.
 Lekner, John (1987). *Theory of Reflection, of Electromagnetic and Particle Waves*. Springer. ISBN 9789024734184.
 MathWorks (2016). Matlab Version R2016b.
 Mosalam, K.M., Takhirov, S.M., and Hashemi, A., 2009. Seismic Evaluation of 1940s Asymmetric Wood-Frame Building Using Conventional Measurements and High-Definition Laser Scanning, *Earthquake Engineering and Structural Dynamics*, 38(10), 1175–1197.
 Mosalam, K.M., Takhirov, S.M., and Park, S. (2014). Applications of Laser Scanning to Structures in Laboratory Tests and Field Surveys. *Journal of Structural Control and Health Monitoring*, Volume 21, Issue 1, pages 115–134, January 2014.
 Takhirov, S.M. (2008). Applications of High-Definition Laser Scanning Technology in Experimental Earthquake Engineering. Presentation at HDS Leica User's Conference.
 Takhirov, S.M. (2010). Laser Scanners in Structural Assessment and FE modeling, 2010 Structures Congress, Orlando, Florida, May 12-15, 2010.
 Trimble (2016). <https://geospatial.trimble.com/sites/geospatial.trimble.com/files/2019-03/Datasheet%20-%20Trimble%20TX6%20Laser%20Scanner%20-%20English%20USL%20-%20Screen.pdf>.